CHAPTER 2

EQUIVALENT CIRCUIT ANALYSIS OF MILO −− REVIEWED

2.1. Introduction

Magnetically insulated line oscillator (MILO) is a crossed field high power microwave (HPM) device closely similar to the linear magnetron and designed specifically to generate giga-watt (GW) level of microwave power in GHz frequency range [Lemke *et al.* (1997), Benford *et al.* (2007)]. The main feature of the MILO is that the DC magnetic field which is required to generate magnetic insulation inside the device is self-induced by the intrinsic electrons flows in the device [Lemke *et al.* (1997), Eastwood *et al.* (1998)]. There is no external circuit required to generate the DC magnetic field, which makes the device compact, lightweight, and highly effective HPM source. The MILO device uses a periodic disk-loaded coaxial structure as a slow-wave structure (SWS) required for beam-wave interactions. To modify the characteristics of the propagating or resonating structures used in the electron beam devices, periodic disc loading or applying corrugation with waveguides has been considered as a well-known practice [Swegle *et al.* (1985), Gilmour (1986)], Lemke *et al.* (1989), Basu (1996), Banna *et al.* (2000), Zhang (2004), Keshri *et al.* (2005), Wang *et al.* (2007), Fan *et al.* (2008), Dwivedi *et al.* (2012), and Dixit *et al.* (2016)]. A cylindrical waveguide with a corrugated inner surface is used as a slow-wave structure for a backward wave oscillator [Swegle *et al.* (1985)]. Azimuthally periodic disc loading can be used as a slow-wave structure for magnetron [Gilmour (1986)]. A coaxial structure with sinusoidal corrugation at the inner surface of the anode is used as an interaction structure or SWS [Lemke *et al.* (1989)]. Azimuthally periodic vanes projecting radially inward from the metal envelope of a helix TWT control the dispersion of the helix and hence widen the bandwidth of the TWT [Jain and Basu (2000)]. Similarly, a circular waveguide with periodic metal disc loading is used as an

interaction structure for gyro-TWT as well as high-power amplifier [Banna *et al.* (2000), Zhang (2004), and Keshri *et al.* (2005)]. The coaxial waveguide structure loaded with axially periodic metal annular discs, and excited in a transverse magnetic (TM) mode, is used as a 'slow-wave' structure of MILO device [Wang *et al.* (2007), Fan *et al.* (2008), Dwivedi *et al.* (2012), and Dixit *et al.* (2016)]. Optimization of the disc parameters provides control over the dispersion relation for further controlling the phase velocity at the desired frequency of RF wave such that maximum beam-wave interaction takes place inside the device.

In the present chapter, an equivalent circuit approach that is followed to study beam wave interaction analysis for the periodic disc loaded coaxial structure used in the MILO device has been revisited. In Section 2.2, various analytical approaches that have been used in analyzing such structures so far have been reviewed. The equivalent circuit analysis for MILO in the beam absent case has been described in section 2.3. The various characteristics of periodic disc loaded coaxial structure such as dispersion relation, phase velocity, and characteristic impedance have been derived using equivalent line parameters in this section. In Section 2.4, the equivalent circuit analysis for MILO in the beam present case has also been presented.

2.2. Reported Analytical Approaches

Any rectangular, circular, or coaxial waveguide periodically loaded with discs may form beam-wave interaction structure periodic in either axial or azimuthal or both directions [Gandhi (1981), Wagner *et al.* (1999), Zhang *et al.* (2003), Wang *et al.* (2010) and Dwivedi *et al.* (2012)]. The electromagnetic analysis of such disc-loaded slow-wave structure can be carried out using field matching theory [Lemke *et al.*

(1989), Zhang *et al.* (2004), and Wang *et al.* (2007)], mode-matching technique [Hahn (1978), Keshri *et al.* (2005) and, Dwivedi *et al.* (2012)] and equivalent circuit approach [Basu (1996), Gandhi (1981), Fan *et al.* (2008), and Dixit *et al.* (2016)].

***(i). Field matching theory*:** The field matching technique has been used by a number of researchers to analyze the characteristics of various associated modes inside the different disc-loaded waveguide structure. For instance, symmetric TM_{01} mode (i.e. transverse magnetic mode) and asymmetric HEM_{11} mode for disc loaded cylindrical structure was analyzed using field matching technique [Wang *et al.* (2005)]. The dispersion function for coaxial disc-loaded SWS has been investigated using field matching theory by Lemke *et al.* (1987) and Zhang *et al.* (2004) but was limited to TM modes only. This technique was also carried out to investigate the dispersion characteristic for both symmetric and asymmetric modes [Wang *et al.* (2007)]. In this technique, the Borgnis function [Zhang and Li (1998)] can be used to express the electromagnetic fields in a different region of the structure (i.e. region *I* as disc free region having space harmonics and region *II* as disc occupied region having standing wave).

***(ii). Mode matching technique*:** The modal matching technique can be used to analyze the characteristics of different disc-loaded and corrugated waveguide structure. For instance, hybrid modes, such as HE_{11} mode was studied using the mode-matching approach for corrugated waveguide structure [Esteban and Rebollar (1991)]. Similarly, the hybrid modes associated with disc-loaded cylindrical waveguide structure was analyzed using this approach [Zhang *et al*. (2003)]. This approach was also used in the analysis of a plasma-filled waveguide excited in the TM mode [Zhang *et al*. (2003)]. Further, this technique was used to analyze the

thick as well as thin metal disc-loaded structure operating in the TE mode [Kesari *et al.* (2004), Kesari *et al.* (2005)]. The metal disc-loaded coaxial waveguide structure excited in fundamental TM mode for MILO was also analyzed using the mode-matching technique [Dwivedi and Jain (2012)]. The mode matching technique considers all the space harmonics in the disc-free region with the structure having axial periodicity and all stationary mode harmonics which is caused by the reflection from disc-walls in the disc occupied region. After applying boundary conditions considering the continuity of fields at the interface of the two regions the dispersion relation is obtained. Further, the relevant field expressions for TM modes in two regions of the structure in a cylindrical coordinate system can be written for non-azimuthally varying modes and under slow-wave consideration.

***(iii). Equivalent Circuit Approach*:** Any disc-loaded waveguide structure can be analyzed by modelling it through its circuit equivalent [Gandhi (1981), Basu (1996), Fan *et al.* (2008), and Dixit *et al.* (2016)]. In the equivalent circuit approach, a period of the structure is treated as a two-terminal circuit network (considering lossless condition) to analyze the characteristics of various slow-wave structures such as helix structure, disc-loaded circular, and coaxial structure, etc. [Watkins (1958), Basu (1996)]. A transmission-line equivalent circuit model was developed to study the effect of periodic disc loading on the structural characteristics of a disc-loaded circular waveguide, which was typically excited in TM_{01} mode [Gallagher (1985)]. Fan *et al.* had used the equivalent circuit approach to analyze the periodic disc-loaded coaxial structure for fundamental modes only [Fan *et al.* (2008)]. They had considered coupling capacitance to find coupling

between corresponding cavities. Furthermore, Dixit and Jain (2016) used equivalent circuit analysis to analyze the symmetric TM_{0n} mode of the coaxial disc-loaded waveguide structure used as an interaction structure for MILO. Thus, the equivalent circuit approach is an alternative approach to characterize the different slow-wave structures (SWS) [Basu (1996)]. This approach treats the SWS as a transmission line which is characterized by a set of four distributed line parameters as shown in Fig. 2.1. The four distributed line parameters are mainly equivalent series inductance per unit length (L_e), equivalent shunt capacitance per unit length (C_e), equivalent series resistance per unit length (R_e), and equivalent shunt conductance per unit length (G_e) of the equivalent transmission line. The propagation characteristics, which are mainly concern with dispersion relation associated with the SWS, can be expressed using these four distributed line parameters. These line parameters include the structure parameters of SWS which resolve whole problems expressed in terms of structural parameters of the SWS. For the sake of simplicity in solving the problem, the losses associated with the structure here are ignored (i.e. considering R_e= 0). To use this approach, the circuit current of n^{th}-section can be written in terms of the circuit voltages of n^{th} -section and $n+1^{th}$ -section. Similarly, the circuit current of the next section (i.e. $n+1^{th}$ – section) can also be written in terms of the same two circuit voltages. At a reference section, these two equations interpret two separate equations relating the circuit current and the circuit voltage. Further, the circuit current and the voltage corresponding to the n^{th}- section which involving the propagation constant of the circuit, can be represented in terms of the corresponding quantity at a reference section with the help of Floquet's theorem. Subsequently, the dispersion relation

of the structure in terms of the line parameters can be derived using the condition for the non-trivial solution of these two equations.

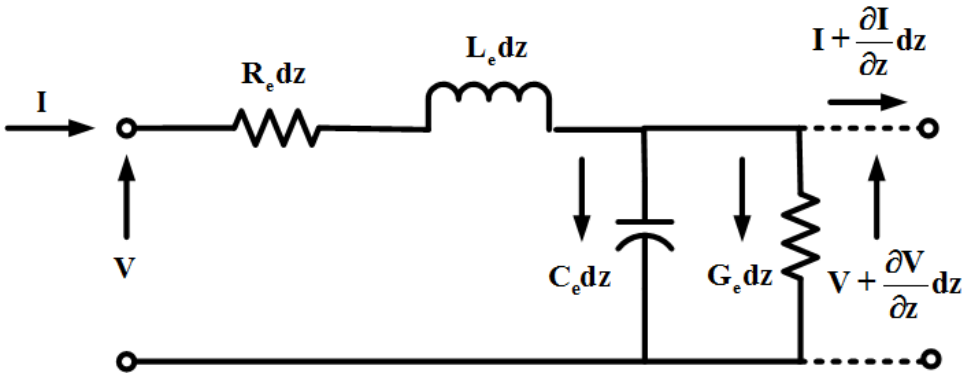

Figure 2.1: The equivalent circuit of transmission line representing the periodic disc loaded coaxial structure for an infinitesimal length *dz*.

2.3. Equivalent Circuit Analysis of the Coaxial Disc loaded RF Interaction Structure for MILO

Equivalent circuit analysis of the MILO device is analyzed here in two cases, the first one is for beam absent case and the second is for beam present case. In the beam absent case, an interaction structure that can be constructed using a disc-loaded coaxial waveguide structure that also forms a slow-wave structure has been analyzed to estimate the potential of RF generation without introducing the actual electron beam at the desired frequency. Whereas, in the beam present case, the estimation of temporal growth rate, RF power, and energy associated with the RF signal at the desired frequency can be evaluated. MILO device uses a metal disc-loaded coaxial structure which is treated as a transmission line and characterized by equivalent line parameters. These line parameters can be derived with the help of the current and voltage telegraphist's equations. Further, these line parameters are expressed in terms of the structure parameters. Finally, the different characteristics like dispersion relation, phase

velocity, and characteristic impedances associated with metal disc-loaded coaxial structure can be derived and represented in terms of the structure parameters. The advantage of the use of the equivalent circuit approach here is that it required only half of the boundary condition at a time and does not require solving a very complex dispersion relation involving $m \times n$ determinants just like required in the field matching approach.

The periodic disc-loaded coaxial structure used in the MILO device is shown in Fig. 2.2. The central cylindrical conductor which having radius r_c is used as a cathode. The outer cylinder is periodically loaded with a metal disc of thickness T and periodicity L, having outer wall radius (r_w) and inner disc radius (r_d) used as an anode. The whole waveguide structure is divided into two regions (i.e. region *I* and region *II*). Region *I* can be called a disc-free region (i.e. region between $r_c < r < r_d$) and support traveling waves whereas region *II* (i.e. region between $r_d < r < r_w$) is termed as disc occupied region and support standing waves.

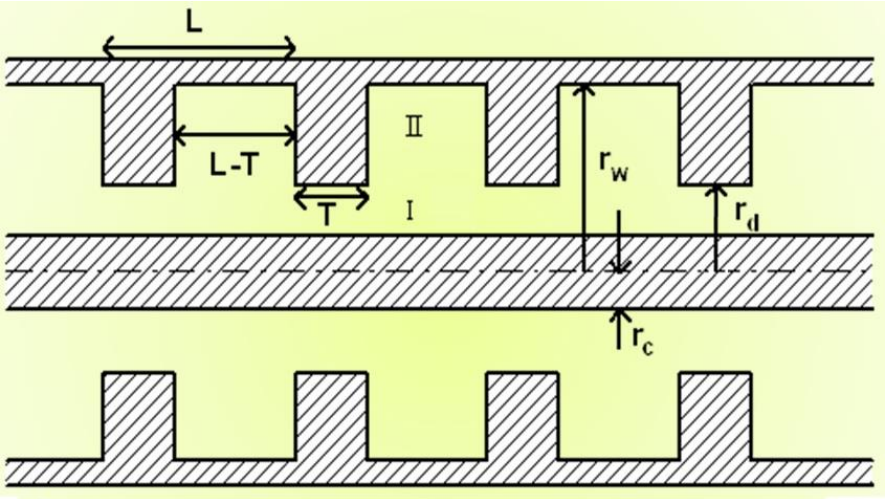

Figure 2.2: The typical schematic view of a periodic disc loaded coaxial structure used as an RF interaction structure for MILO.

2.3.1. EM Field Expressions and Boundary Conditions

As far as exploring RF interaction structures for MILO is concerned, Dixit and Jain (2016) found it worth trying out the equivalent circuit approach (Section 2.2) to study the behavior of a periodic disc-loaded coaxial waveguide with respect to its dispersion characteristics and hence predict the optimum structure parameters for efficient beam-wave interaction at the desired frequency. The same approach is also adapted in the work presented in this thesis, however, with due care to include the rigor of considering the effect of azimuthal partitioning (i.e. two-dimensional periodicity) in the analysis for the possibility of bi-frequency generation through a single MILO device. The present section is dedicated to presenting the basic field expressions and electromagnetic boundary conditions to be used in the Chapters of the thesis to follow, for the analysis of an azimuthally partitioned axially periodic metal disc-loaded coaxial waveguide structure.

2.3.1.1. Field Expression in the disc-free region (i.e. region *I*: $r_c \le r \le r_d$)

The electric and magnetic field component for periodic disc loaded coaxial structure in the disc-free region as shown in Fig. 2.2 for symmetric TM mode can be written in the cylindrical coordinate system as [Dwivedi and Jain (2012), Dixit and Jain (2016)]:

$$E_z^I = \sum_{n=-\infty}^{\infty} [A_n^I J_0\{\gamma_n^I r\} + B_n^I Y_0\{\gamma_n^I r\}] \exp j(\omega t - \beta_n^I z) \tag{2.1}$$

$$E_r^I = \sum_{n=-\infty}^{\infty} \frac{j\beta_n^I}{\gamma_n^I} [A_n^I J_1\{\gamma_n^I r\} + B_n^I Y_1\{\gamma_n^I r\}] \exp j(\omega t - \beta_n^I z) \tag{2.2}$$

$$H_\theta^I = j\omega\varepsilon \sum_{n=-\infty}^{\infty} \frac{1}{\gamma_n^I} [A_n^I J_1\{\gamma_n^I r\} + B_n^I Y_1\{\gamma_n^I r\}] \exp j(\omega t - \beta_n^I z) \quad . \tag{2.3}$$

Here, Superscript (*I*) is used to refer to the region *I*, the disc-free region, and $\beta_n^I = \beta_0^I \pm 2n\pi / L$ is the axial propagation constant which utilizing Floquet's theorem because of the periodicity in the structure. The radial propagation constant is represented by γ_n^I $(=(k^2 - \beta_n^{I^2})^{1/2})$ and k $(=\omega(\mu_0\varepsilon_0)^{1/2})$ representing free space propagation constant. In region-*I*, the space harmonics is presented by whole number *n* (i.e. *n* = 0, ±1, ±2, ±3, …) A_n^I and B_n^I are the unknown constants to be determined for deriving dispersion relation. J_0 and J_1 represents the Bessel functions of 1st kind and Y_0, Y_1 as Bessel functions of 2nd kind for zeroth and first order, respectively having an argument as radial propagation constant as $\gamma_n^I r$.

2.3.1.2. Field Expression in disc occupied region (i.e. region *II*: $r_d \le r \le r_w$)

The region between two consecutive discs (i.e. region *II*) which is shown in Fig. 2.2, supports stationary waves due to reflection at discs in this region. The supported stationary waves in the disc-occupied region creates modal harmonics, represented by natural numbers *m* (i.e. *m* = 1, 2, 3,…). The axial electric and azimuthal magnetic field expression for symmetric TM mode supported in this region, which define the stationary wave, is written as [Dwivedi and Jain (2012), Dixit and Jain (2016)]:

$$E_z^{II} = \sum_{m=1}^{\infty} A_m^{II} \, X_0\{\gamma_m^{II} r\} \exp(j\omega t) \sin(\beta_m^{II} z) \tag{2.4}$$

$$E_r^{II} = \sum_{m=1}^{\infty} \frac{j\beta_m^{II}}{\gamma_m^{II}} A_m^{II} X_0'\{\gamma_m^{II} r\} \exp(j\omega t) \sin(\beta_m^{II} z) \tag{2.5}$$

$$H_\theta^{II} = \sum_{m=1}^{\infty} \frac{j\omega\varepsilon}{\gamma_m^{II}} A_m^{II} X_0'\{\gamma_m^{II} r\} \exp(j\omega t) \sin(\beta_m^{II} z) \tag{2.6}$$

Here, A_m^{II} is the unknown constant of EM field component, superscript (*II*) used to refer to the disc occupied region, $\beta_m^{II} = m\pi/(L-T)$ is the axial propagation constant, and γ_m^{II} $(=(k^2-\beta_m^{I^2})^{1/2})$ is the radial propagation constant for this region. The component X_0 and it's derivative which is represented by the prime or X_0' are the functions of Bessel's function defined as:

$$X_0\{\gamma_m^{II} r\} = Y_0\{\gamma_m^{II} r_w\} J_0\{\gamma_m^{II} r\} - J_0\{\gamma_m^{II} r_w\} Y_0\{\gamma_m^{II} r\}$$

$$X_0'\{\gamma_m^{II} r\} = Y_0\{\gamma_m^{II} r_w\} J_1\{\gamma_m^{II} r\} - J_0\{\gamma_m^{II} r_w\} Y_1\{\gamma_m^{II} r\}$$

2.3.1.3. Boundary Conditions

In order to characterize a periodic disc-loaded coaxial waveguide, the field expressions for the waveguide, excited in azimuthally symmetric TM modes ($H_z = 0$), developed in previous sections (Section 2.3.1.1 and Section 2.3.1.2), need to be combined with the relevant electromagnetic boundary conditions. The electromagnetic boundary conditions stating the continuity of the tangential components of electric and magnetic field intensities at the interface, $r = r_d$, between the free-space disc-free region (i.e. region *I*) and disc-occupied free-space region (i.e. region *II*) (Fig. 2.2) as well as the vanishing of the axial component of electric field intensity at the metal inner circumferential edge of the discs, $r = r_d$, may be written as:

$$E_z^I = \begin{cases} E_z^{II} & 0 < z < (L-T) \\ 0 & (L-T) \le z \le L \end{cases} \qquad (r = r_d) \qquad (2.7)$$

$$E_z^I = 0 \qquad 0 < z < \infty \qquad (r = r_c) \qquad (2.8)$$

$$H_{\theta}^{I} = H_{\theta}^{II} \qquad 0 < z < (L-T) \qquad (r = r_d) \quad . \qquad (2.9)$$

The discontinuity at the interface of the two regions causes the discontinuation of the tangent (i.e. azimuthal) component of the magnetic field intensity (H_{θ}), which is equal to the surface current density (J_z) and is written as [Dixit and Jain (2016)]:

$$H_{\theta}^{II} - H_{\theta}^{I} = J_z \qquad 0 \le z < (L-T) \qquad (r = r_d) \quad . \qquad (2.10)$$

Similar to the azimuthal magnetic field intensity, the radial components of electric field intensity are discontinuous at the interface between two regions. This discontinuity amount can be evaluated by equating it with the ratio of surface charge density to the dielectric constant (i.e. ρ_s / ε) and is written as [Dixit and Jain (2016)]:

$$E_{r}^{II} - E_{r}^{I} = \rho_s / \varepsilon \qquad 0 \le z < (L-T) \qquad (r = r_d) \quad . \qquad (2.11)$$

2.3.2. Equivalent Line Parameters

The EM field expressions for the two regions (i.e. region *I* and region *II*) and the boundary conditions which have been explained in the previous sections used to obtain the equivalent line parameters (i.e. shunt capacitance per unit length (C_e) and series inductance per unit length (L_e)). To derive the expression for these line parameters, the unknowns present in the expressions (i.e. A_n^I , B_n^I , and A_m^{II}) have to be eliminated using the boundary conditions. Further, the phase velocity, dispersion relation, and the characteristic impedance of the structure are evaluated using these equivalent circuit line parameters that are handy and easy to process throughout.

2.3.2.1. Equivalent shunt capacitance per unit length

The current Telegraphist's equation of the equivalent transmission line here can be used to find the equivalent shunt capacitance per unit length for the interaction structure [Kartikeyan *et al*. (1992), Basu (1996), Dixit and Jain (2016)]:

$$\frac{\partial I_z}{\partial z} + C_e \frac{\partial V}{\partial t} = 0 \qquad . \tag{2.12}$$

Replacing $\partial / \partial z$ with $-j\beta_n^I$ and $\partial / \partial t$ with $j\omega$ and rearranging the above equation (i.e. Eqs. (2.12)) can be written as:

$$C_e = \frac{\beta_n^I}{\omega} \frac{I_z}{V} \qquad . \tag{2.13}$$

Here, I_z is the axial current which can be evaluated by the axial current density for a unit length of structure such as [Dixit and Jain (2016)]:

$$J_z = I_z / 2\pi r_d \tag{2.14}$$

To find the relation between field constants presents in the EM field components of the region *I*, (i.e. A_n^I and B_n^I), the above boundary condition (2.8) is applied and the relation can be expressed as:

$$B_n^I = -\frac{J_0\{\gamma_n^I r_c\}}{Y_0\{\gamma_n^I r_c\}} A_n^I \qquad . \tag{2.15}$$

Similarly, the relationship between field constants A_n^I and A_m^{II} can be obtained by substituting the EM field expression given in Eqs. (2.1) and (2.4) in the first boundary condition given in Eqs. (2.7) and the relation is given as:

$$\sum_{n=-\infty}^{\infty}[V_0\{\gamma_n^I r\}]\exp j(\omega t-\beta_n^I z)=\sum_{m=1}^{\infty}A_m^{II}X_0\{\gamma_m^{II}r\}\exp(j\omega t)\sin(\beta_m^{II}z)\ , \qquad (2.16)$$

here, $V_0\{\gamma_n^I r\}=A_n^I J_0\{\gamma_n^I r\}+B_n^I Y_0\{\gamma_n^I r\}$.

For the sake of simplicity of the calculation, the time effect has been eliminated from the above equation. Further, to remove the axial distance *z* from the above Eqs. (2.16), $\sin(\beta_m^{II}z)$ has been multiplied on both sides of the expression and the resultant is integrated within the limit $0\le z\le L-T$, which finally give the expression [Dwivedi and Jain (2012) and Dixit and Jain (2016)]:

$$A_m^{II}=\sum_{n=-\infty}^{\infty}U_{n,m}A_n^I \qquad (2.17)$$

with, $U_{n,m}=\left(\frac{2\beta_m^{II}}{L-T}\right)\left(\frac{(-1)^m\exp(j\beta_n^I(L-T))-1}{\beta_m^{II^2}-\beta_n^{I^2}}\right)\left(\frac{X_0\{\gamma_m^{II}r\}}{Z_0\{\gamma_n^I r\}}\right)$ and,

$$Z_0\{\gamma_n^I r\}=Y_0\{\gamma_n^I r_c\}J_0\{\gamma_n^I r\}-J_0\{\gamma_n^I r_c\}Y_0\{\gamma_n^I r\}\ .$$

Similarly, multiplying $\sin(\beta_m^{II}z)$ on both sides of boundary condition (2.10) and integrating the expression on both sides within the limit $0\le z\le L-T$, the field constant A_n^I can be represented in terms of circuit current which can be expressed as:

$$A_n^I=R_{nm}\{\gamma_n^I r\}I_z \ , \qquad (2.18)$$

here,

$$R_{nm}\{\gamma_n^I r\}=\frac{\gamma_n^I\gamma_m^{II}Y_0\{\gamma_n^I r_c\}Z_0\{\gamma_n^I r\}\cos(\beta_m^{II}(L-T))\exp(-j\omega t)}{2j\omega\varepsilon\pi r_d[\beta_m^{II}X_0\{\gamma_m^{II}r_d)X_0'\{\gamma_m^{II}r_d\}Y_0\{\gamma_n^I r_c\}-\gamma_m^{II}J_1\{\gamma_n^I r_d\}Z_0\{\gamma_n^I r\}]S}$$

and, $S=\left(\frac{2\beta_m^{II}}{L-T}\right)\left(\frac{(-1)^m\exp(j\beta_n^I(L-T))-1}{(\beta_m^{II})^2-(\beta_n^I)^2}\right)$.

By substituting B_n^I and A_n^I given in the above expression (2.15) and (2.18) respectively, into the expression (2.1), the axial electric field intensity (E_z^I) can be expressed in terms of axial current such as:

$$E_z^I = \sum_{n=-\infty}^{\infty} P_{nm} I_z \quad , \tag{2.19}$$

here, $P_{nm} = \sum_{n=-\infty}^{\infty} R_{nm}\{\gamma_n^I r\} Z_0\{\gamma_n^I r_d\}$.

The axial electric field intensity E_z can be represented in the form of the scalar and vector circuit potential [Basu (1996)] as:

$$E_z = -\frac{\partial V}{\partial z} - \frac{\partial A_z}{\partial t} \quad . \tag{2.20}$$

By substituting $\partial/\partial z$ with $-j\beta_n^I$ and $\partial/\partial t$ with $j\omega$ in the above Eqs. (2.20) can be rewritten as:

$$E_z = j\beta_n V - j\omega A_z \quad . \tag{2.21}$$

The relation between vector potential A_z and scalar potential V in the cylindrical coordinate system can be given as:

$$\frac{\partial A_z}{\partial z} + \mu\varepsilon \frac{\partial V}{\partial t} = 0 \quad , \tag{2.22}$$

which can be further rewritten just like Eqs. (2.21) as:

$$-j\beta_n A_z + j\omega\mu\varepsilon V = 0 \quad . \tag{2.23}$$

Substituting the Eq. (2.23) into Eq. (2.21), the axial electric field intensity E_z can be expressed in term of scalar potential V and expressed as:

$$E_z^I = j\left(\frac{(\gamma_n^I)^2}{\beta_n^I}\right) V \quad . \tag{2.24}$$

Finally, the axial current to voltage ratio (i.e. I_z / V) can be obtained using the above Eqs. (2.19) and (2.24) which is further substituted in the Eq. (2.13) to calculate the equivalent capacitance per unit length and expressed as:

$$C_e = \frac{j(\gamma_n^I)^2}{\omega} \frac{1}{P_{nm}} \quad . \tag{2.25}$$

2.3.2.2. Equivalent series inductance per unit length

Similar to the equivalent shunt capacitance, the voltage Telegraphist's equation of the equivalent transmission line can be used to find the equivalent series inductance per unit length for this RF interaction structure [Basu (1996), Dixit and Jain (2016)]:

$$\frac{\partial V}{\partial z} + L_e \frac{\partial I_\theta}{\partial t} = 0 \quad . \tag{2.26}$$

According to the similar explanation given in the previous subsection, the expression (2.26) can be rewritten as:

$$L_e = \left(\frac{\beta_n}{\omega} \right) \frac{V}{I_\theta} \quad . \tag{2.27}$$

The ratio of circuit potential to the circuit current as given in expression (2.27) can be derived following a similar process as explained in the previous subsection (i.e. subsection 2.3.2.1). For this, the EM field expression used in the Eqs. (2.3) and (2.6) are substituted in boundary condition (2.9) and multiplied $\sin(\beta_m^{II} z)$ on both sides followed by integration of the expression within the limit $0 \le z < (L - T)$. The final expression shows the relation between field constant A_m^{II} and A_n^I which is expressed as:

$$A_m^{II} = \sum_{n=-\infty}^{\infty} X_{n,m} A_n^I \quad , \tag{2.28}$$

here,

$$X_{n,m} = \left(\frac{2\beta_m^{II}}{L-T} \times \frac{(-1)^m \exp(\mathrm{j}\beta_n^I(\mathrm{L}-\mathrm{T})) - 1}{\beta_m^{II^2} - \beta_n^{I^2}} \right) \left(\frac{Z_0'\{\gamma_n^I r\}}{X_0'\{\gamma_m^{II} r\} Y_0\{\gamma_n^I r_c\}} \right) \frac{\gamma_m^{II}}{\gamma_n^I} .$$

To find the relation between field constant A_n^I and the azimuthal circuit current I_θ, the boundary condition (2.11) multiplied $\sin(\beta_m^{II} z)$ on both sides and integrated within the limit $0 \le z < (L-T)$ expressed as:

$$\int_0^{(L-T)} (E_r^{II} - E_r^I) \sin(\beta_m^{II} z)\, dz = \int_0^{(L-T)} \frac{\rho_s}{\varepsilon} \sin(\beta_m^{II} z)\, dz = \int_0^{(L-T)} \frac{I_\theta}{(2\pi r_d)\varepsilon} \sin(\beta_m^{II} z)\, dz \quad . \quad (2.29)$$

Substituting the radial electric field components from Eqs. (2.2) and (2.5) into Eq. (2.29) and after rearranging the above expression the relation between field constant A_n^I and azimuthal current I_θ can be obtained, which can be given as:

$$A_n^I = \sum_{n=-\infty}^{\infty} Q_{nm} I_\theta \quad , \quad (2.30)$$

where,

$$Q_{nm} = \frac{\gamma_n^I \gamma_m^{II} Y_0\{\gamma_n^I r_c\} \cos(\beta_m^{II}(L-T))}{j2\pi\varepsilon r_d [\beta_m^{II} \gamma_n^I Z_0'\{\gamma_n^I r_d\} - \beta_n^I \gamma_m^{II} Z_0'\{\gamma_n^I r\}] S \exp(-j\omega t)} .$$

Further, the field constant value obtained from Eq. (2.30) substituted in Eq. (2.1) to obtain the relation between electric field intensity and the azimuthal current which can be written as:

$$E_z^I = W_{nm} I_\theta \quad (2.31)$$

here,

$$W_{nm} = \frac{\gamma_n^I \gamma_m^{II} Z_0\{\gamma_n^I r_d\} \cos(\beta_m^{II}(L-T))}{j2\pi\omega\varepsilon r_d [\beta_m^{II} \gamma_n^I Z_0'\{\gamma_n^I r_d\} - \beta_n^I \gamma_m^{II} Z_0'\{\gamma_n^I r\}] S}$$

Finally, after equating the Eq. (2.24) with Eq. (2.31), the ratio of circuit potential to the azimuthal circuit current can be obtained which is further substituted into the Eq. (2.27) to find the equivalent series inductance per unit length which can be expressed as:

$$L_e = \frac{1}{j\omega}\left(\frac{\beta_n}{\gamma_n^I}\right)^2 W_{nm} \quad . \tag{2.32}$$

2.3.3. Dispersion Relation:

The dispersion relation of the axially periodic disc-loaded coaxial waveguide structure used in MILO device in the absence of an electron beam or the 'cold' dispersion relation can be used to obtain the axial phase propagation constant of the structure hence the $\omega - \beta$ characteristics of the structure and the effect of the disc parameters on the shape of such characteristics. The dispersion relation can be obtained using the above derived equivalent line parameters (i.e. equivalent shunt capacitance per unit length and equivalent series inductance per unit length) and the expression given as [Basu (1996), Dixit and Jain (2016)]:

$$\beta^2 - \omega^2 L_e C_e = 0 \quad . \tag{2.33}$$

After substituting the expressions (2.25) and (2.32) into the expression (2.33), the dispersion relation can be expressed in terms of structure parameters which after rearranging become similar to the dispersion relation expression obtained using the field matching technique. The dispersion relation obtained using the field matching technique can be written as [Dwivedi and Jain (2012)]:

$$\sum_{n=-\infty}^{\infty}\left[\left(\frac{X_0\{\gamma_m^{II} r\}}{Z_0\{\gamma_n^I r\}}\right)S - \left(\frac{\gamma_m^{II}}{\gamma_n^I}\right)\left(\frac{Z_0'\{\gamma_n^I r\}}{Y_0\{\gamma_n^I r_c\}X_0'\{\gamma_m^{II} r\}}\right)S\right] = 0 \quad (m = 1, 2, 3, ...)$$

2.3.4. Characteristic Impedance

The characteristic impedance of the periodic disc-loaded coaxial structure can help in matching the impedance of the structure at the different subsections which will explain in detail in the next chapter (i.e. Chapter 3). This is also an important tool to obtain the optimum design parameters of the structures. The expression for the characteristic impedance of the structure can be obtained by substituting the equivalent line parameters in the expression given as [Basu (1996), Dixit and Jain (2016)]:

$$Z_0 = (L_e / C_e)^{1/2} \tag{2.34}$$

2.3.5. Phase Velocity

The phase velocity of normal modes along the waveguide is always greater than the velocity of light. To reduce this phase velocity for efficient beam-wave interaction inside the slow-wave devices, like MILO, the corrugation inside the waveguide is designed or periodic disc loading is performed in the coaxial waveguide structure. Thus, the phase velocity is a very important parameter to design any slow-wave structure. The expression for phase velocity for periodic structure can be obtained in the form of equivalent line parameters and written as [Basu (1996), Dixit and Jain (2016)]:

$$v_p = 1/(L_e C_e)^{1/2} \tag{2.35}$$

2.4. Equivalent Circuit Analysis in Presence of the Electron Beam

In the previous section, the RF interaction section of the MILO device which is formed with the periodic disc loading inside the coaxial waveguide structure has been analyzed in the absence of an electron beam using an equivalent circuit approach. The analysis

mainly derives the dispersion relation, phase velocity, and characteristic impedance using equivalent line parameters which involve the device design parameters to perfectly characterize the interaction structure. Further, to analyze the process of beam-wave interaction and estimate the RF energy stored in the interaction structure can be performed using the equivalent circuit approach in this section. The application of this approach starts with consideration of relativistic Brillouin flow of the electron beam which helps in finding the space charge equilibrium involve with the electron beam presence in the structure [Dixit (2017)].

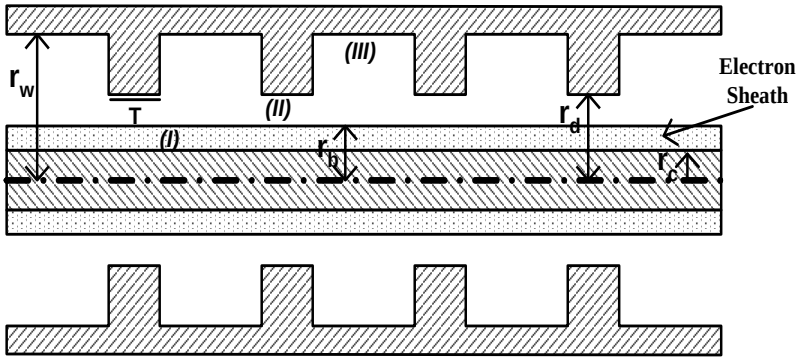

Figure 2.3: The typical schematic view of periodic disc-loaded coaxial waveguide structure with an electron beam.

The electromagnetic (EM) field associated with the beam presence region inside the device can be calculated using the linearized Vlasov-Maxwell's equation [Dwivedi and Jain (2012) and Lemke (1989)]. The relevant EM field associated with other regions of the device is derived considering the effect of beam presence region which is further substituted in the boundary condition to obtain a set of simultaneous equations. The dispersion relation in the presence of the electron beam can be obtained by solving these simultaneous equations. Further, the temporal growth rate, RF energy stored, and

transfer through the slow-wave structure is calculated using an equivalent circuit approach [Dixit (2017)]. These parameters are evaluated to investigate the oscillation condition inside the RF structure. For further rigorous and simplicity, here equivalent circuit approach is preferred.

2.4.1. Analysis

In this section, the analysis of periodic disc-loaded coaxial waveguide structure shown in Fig. 2.3 is extended, by taking into account the presence of beam due to explosive emission from the cathode surface. The whole structure is divided into three regions, considering region *I* as beam presence section, region *II* as disc-free traveling wave supporting section, and region *III* as disc occupied standing wave supporting section. A high voltage applied between anode and cathode resulting strong electric field at the cathode which forms plasma on the cathode surface due to the surface flashover mechanism. The enhanced electric field then extracts a space-charge limited electron flow from this plasma [Miller (1998)]. The present work is extended considering the perturbation effect due to axial periodicity of discs, to estimate the mechanism of energy exchange between an electron beam and RF. During analysis consider a region of plasma (electron sheath) in equilibrium, but when this region is perturbed, space charge waves are formed due to periodicity of discs and results in space charge instability. The axial periodic metal boundary of the anode structure will affect the outer radius of the electron sheath due to the presence of radial field components. Axial field component perturbs space charge equilibrium. Here, considering that coaxial discs oscillate at TM mode. Corresponding to this mode, three nonzero field components are radial electric field E_r , axial electric field E_z , and azimuthal magnetic field B_θ . Taking into account

space-charge waves, the correlation between particles and different field components can be described using a linearized Vlasov-Maxwell equation as:

$$\left.\begin{aligned} &\frac{\partial E_{r1}}{\partial z}-\frac{\partial E_{z1}}{\partial r}=-\frac{1}{c}\frac{\partial B_{\theta 1}}{\partial t} \\ &-\frac{\partial B_{\theta 1}}{\partial z}=\frac{1}{c}\frac{\partial E_{r1}}{\partial t} \\ &-\frac{1}{r}\frac{\partial}{\partial z}rB_{\theta 1}=\frac{4\pi}{c}J_{z1}+\frac{1}{c}\frac{\partial E_{z1}}{\partial t} \end{aligned}\right\} \quad . \tag{2.36}$$

Here J_{z1} represents the perturbed (RF) axial current density,

$$J_{z1}\{x,t\}=-e\int v_b f_1\{x,p,t\}dp \ .$$

The above equation $f_1\{x,p,t\}$ represents RF distribution function and can be expressed using floquet's theorem and Vlasov equation as [Lemke *et al.* (1997)]:

$$f_1\{x,p,t\}=ie\frac{\partial f_0}{\partial p_z}\sum_{n=-\infty}^{\infty}\frac{E_{z,n}}{\zeta_n}\exp\left[i\left(\beta_n z-\omega t\right)\right],$$

where $\zeta_n=\omega-v_b\beta_n$ represents velocity shifted frequency. Different relevant EM field intensities components can be expressed by substituting Maxwell-Vlasov equations into the Vlasov equation in conjunction with Floquet theorem [Lemke (1989)]:

The different components of *EM* field intensities, $E_{r,n}$, $E_{z,n}$, and $H_{\Theta,n}$, can be expressed as [Lemke(1989)]:

$$\left(\frac{1}{r}\frac{d}{dr}r\frac{d}{dr}+\Gamma_n^{*2}\right)E_{z,n}=0 \ , \tag{2.37}$$

$$E_{r,n}=j\frac{\beta_n}{\gamma_n^2}\frac{dE_{z,n}}{dr}, \tag{2.38}$$

$$H_{\theta,n}=j\frac{k}{\gamma_n^2}\frac{dE_{z,n}}{dr} \ , \tag{2.39}$$

where $\Gamma_n^{*2} = \gamma_n^{\,2}/[1-(\omega_p^{\,2}/\gamma_0^{\,3}\zeta_n^2)]$ represents constant in terms of the beam parameter and $\gamma_n^{\,2} = \frac{\omega^2}{c^2} - \beta_n^{\,2}$ is the radial propagation constant; $\beta_n = \beta_0 + nh_0$ is the axial propagation constant and $\omega_p\ (=(4\pi e\rho/m)^{1/2})$ is electron plasma frequency. Differential form of the field expression (2.37) can be solved with the help of making some relevant assumptions, e.g., the transverse electron motion in the perturbed state is negligible compared to corresponding axial motion. Thus, the expression for the axial electric field, in the presence of beam, can be evaluated by solving the second-order differential equation using a formulation of singular point transformation and Taylor series [Dwivedi and Jain (2013)]:

$$E_{z,n} = A_n J_n\{G_{2,n} r\} + B_n Y_n\{G_{2,n} r\}, \tag{2.40}$$

where, $G_{2,n} = (\Gamma_n^* r/\xi)^2 - 1/3.$

(i). EM field expressions in the region *I*

The region between the coaxial cylindrical cathode and the outer radius of an electron beam is considered as region I. Travelling RF waves with all space harmonics are considered to be present in this region. Considering Eq. (2.40), the expression for the axial component can be written as [Dwivedi and Jain (2012)]:

$$E_z^I = \sum_{n=-\infty}^{n=\infty} J_0\{G_{2n} r\} A_n^I e^{j\beta_n z}\ , \tag{2.41}$$

$$E_r^I = -j \sum_{n=-\infty}^{n=\infty} \frac{\beta_n G_{2,n}}{\gamma_n^2} J_1\{G_{2,n}\} \mathrm{A}_n^I\, e^{j\beta_n z}, \tag{2.42}$$

$$H_\theta^I = -j\omega\varepsilon \sum_{n=-\infty}^{n=\infty} \frac{G_{2,n}}{\gamma_n^2} J_1\{G_{2,n}\,\mathrm{r}\} A_n^I e^{j\beta_n z}\,. \tag{2.43}$$

(ii). EM field expressions in region *II*:

The field expression for region II can be written as [Dwivedi and Jain (2012)]:

$$\left.\begin{aligned} E_z^{II} &= -\sum_{n=-\infty}^{n=\infty} \varphi_n[((1-bJ_0\{\gamma_n r_b\}Y_0\{\gamma_n r_b\})J_0\{\gamma_n r\}+bJ_0^2\{\gamma_n r_b\}Y_0\{\gamma_n r\})]A_n^I e^{j\beta_n z} \\ E_r^{II} &= j\sum_{n=-\infty}^{n=\infty}\left[\frac{\varphi_n\beta_n}{\gamma_n^2}((1-bJ_0\{\gamma_n r_b\}Y_0\{\gamma_n r_b\})J_1\{\gamma_n r\}+bJ_0^2\{\gamma_n r_b\}Y_1\{\gamma_n r\})\right]A_n^I e^{j\beta_n z} \\ H_\theta^{II} &= -j\omega\varepsilon\sum_{n=-\infty}^{n=\infty}\frac{\phi_n}{\gamma_n}[(1-bJ_0\{\gamma_n r_b\}Y_0\{\gamma_n r_b\})J_1\{\gamma_n r\}+bJ_0^2\{\gamma_n r_b\}Y_1\{\gamma_n r\}]A_n^I e^{j\beta_n z} \end{aligned}\right\} \quad , \ (2.44)$$

where, I_b is beam current, $\varphi_n = Y_0\{G_{2,n}r\}/J_0\{G_{2,n}r\}$ and $b = c^2(k^2-\beta_n^2/(\omega-\gamma_n\upsilon_b))^2 I_b$.

(iii). EM field expression in region *III*:

The axial electric field intensity and azimuthal magnetic field in region *III* for the stationary wave supported between discs can be written as [Dwivedi and Jain (2012)]:

$$E_z^{III} = \sum_{m=1}^{\infty} E_{z,m}^{III} = \sum_{m=1}^{\infty} X_0\{\gamma_m^{III} r\}A_m^{III}\exp(j\omega t)\sin\beta_m^{III} z\,, \qquad (2.45)$$

where, $X_0\{\gamma_m^{III} r\} = Y_0\{\gamma_m^{III} r_w\}J_0\{\gamma_m^{III} r\} - J_0\{\gamma_m^{III} r_w\}Y_0\{\gamma_m^{III} r\}$.

$$E_r^{III} = \sum_{m=1}^{\infty}\frac{j\beta_m^{III}}{\gamma_m^{III}}A_m^{III}X_0'\{\gamma_m^{III} r\}\exp(j\omega t)\sin(\beta_m^{III} z)\,, \qquad (2.46)$$

$$H_\theta^{III} = \sum_{m=1}^{\infty} H_{\theta,m}^{III} = \sum_{m=1}^{\infty} A_m^{III}X_0'\{\gamma_m^{III} r\}\exp(j\omega t)\sin(\beta_m^{III} z)\,, \qquad (2.47)$$

where, $X_0'\{\gamma_m^{III} r\} = Y_0\{\gamma_m^{III} r_w\}J_1\{\gamma_m^{III} r\} - J_0\{\gamma_m^{III} r_w\}Y_1\{\gamma_m^{III} r\}$.

(iv). Boundary Conditions

Just like the above boundary condition explained in the absence of an electron beam, the boundary condition in the presence of an electron beam is divided into two parts. One

part representing the discontinuity of two regions between region *I* and *II* and the other represent the discontinuity between region *II* and *III*, respectively.

Thus, the boundary condition between region *I* and *II* can be given as:

$$E_z^I = \begin{cases} E_z^{II} & 0 < z < (L-T) \\ 0 & (L-T) \le z \le L \end{cases} \qquad (r = r_b) \qquad (2.48)$$

$$E_z^I = 0 \qquad 0 < z < \infty \qquad (r = r_c) \qquad (2.49)$$

$$H_\theta^I = H_\theta^{II} \qquad 0 < z < (L-T) \qquad (r = r_b) \quad . \qquad (2.50)$$

Similarly, the boundary condition between region *II* and *III* can be given as:

$$E_z^{II} = \begin{cases} E_z^{III} & 0 < z < (L-T) \\ 0 & (L-T) \le z \le L \end{cases} \qquad (r = r_d) \quad , \qquad (2.51)$$

$$H_\theta^{II} = H_\theta^{III} \qquad 0 < z < (L-T) \qquad (r = r_d) \quad . \qquad (2.52)$$

The discontinuity at the interface of the two regions causes the discontinuation of the tangent (i.e. azimuthal) component of the magnetic field intensity (H_θ), which is equal to the surface current density (J_z) and is written as [Dixit (2016)]:

$$H_\theta^{III} - H_\theta^{II} = J_z \qquad 0 \le z < (L-T) \qquad (r = r_d) \quad . \qquad (2.53)$$

Similar to the azimuthal magnetic field intensity, the radial components of electric field intensity are discontinuous at the interface between two regions. This discontinuity amount can be evaluated by equating it with the ratio of surface charge density to the dielectric constant (i.e. ρ_s / ε) and can be written as [Dixit (2016)]:

$$E_r^{III} - E_r^{II} = \rho_s / \varepsilon \qquad 0 \le z < (L-T) \qquad (r = r_d) \quad . \qquad (2.54)$$

(v). Equivalent Shunt Capacitance

The expression for the equivalent shunt capacitance per unit length in the presence of the electron beam can be derived similarly to that in the absence of an electron beam as explained in the above section. The final expression for beam presence equivalent shunt capacitance per unit length is given as [Dixit (2016)]:

$$C_e^*\{\gamma_n r\} = \frac{j}{\omega}\left[\frac{(\gamma_n^I)^2}{P_{nm}^*\{\gamma_n r\}}\right] \quad , \tag{2.55}$$

where star (*) marks indicate the beam presence case and P_{mn}^* is considered as the capacitance factor expressed as:

$$P_{nm}^*\{\gamma_n r\} = \sum_{n=-\infty}^{\infty} R_{nm}^*\{\gamma_n r\} J_0\{G_{2n} r_c\}$$

where, $R_{nm}^*\{\gamma_n r\} = \sum_{n=-\infty}^{\infty} \frac{X_0\{\gamma_m^{III} r\}\gamma_m^{III}(L-T)^2\cos(\beta_m^{III}(L-T))}{2\pi r_d S(j\omega\varepsilon)\left[B_1\{\gamma_n r\}X_0'\{\gamma_m^{III} r\} + X_0\{\gamma_m^{III} r\}\gamma_m^{III}(L-T)^2 B_2\{\gamma_n r\}\right]}$,

$$B_1\{\gamma_n r\} = -\sum_{n=-\infty}^{\infty} \phi_n\left[[(1-bJ_0\{\gamma_n r_b\}Y_0\{\gamma_n r_b\})J_0\{\gamma_n r\} + bJ_0^2\{\gamma_n r_b\}Y_0\{\gamma_n r\}]\right], \text{ and}$$

$$B_2\{\gamma_n r\} = \phi_n / \gamma_n\left[(1-bJ_0\{\gamma_n r_b\}Y_0\{\gamma_n r_b\})J_1\{\gamma_n r\} + bJ_0^2\{\gamma_n r_b\}Y_1\{\gamma_n r\}\right].$$

(vi). Equivalent Series Inductance:

The equivalent series inductance per unit length in the presence of an electron beam can be derived as similar to that in the absence of an electron beam as explained in the above section. The final expression for beam presence equivalent series inductance per unit length is given as [Dixit (2016)]:

$$L_e^*\{\gamma_n^I r\} = \frac{1}{j\omega}\left(\frac{\beta_n}{\gamma_n^I}\right)^2 Q_{nm}^*\{\gamma_n^I r\} J_0\{G_{2n} r\} \quad , \tag{2.56}$$

where star (*) marks indicate the beam presence case and Q_{mn}^{*} is considered as the inductance factor expressed as:

$$Q_{nm}^{*}\left\{\gamma_n^I r\right\} = \frac{\cos(\beta_m^{II}(L-T))\gamma_n(L-T)}{4\pi r_d \varepsilon(L-T)[(-jB_2\left\{\gamma_n r\right\} S)]}$$

with,
$$S = \left\{\frac{\beta_m^{III}(1-(-1)^m \exp j\beta_n^I(L-T))}{\left(\beta_m^{III}\right)^2 - (\beta_n^I)^2}\right\}.$$

(vii). Dispersion relation and Temporal Growth Rate

The dispersion relation is used for investigating the electromagnetic behavior of the oscillation region for the RF interaction region of the MILO structure in the presence of the electron beam and is written as:

$$\beta = \omega\sqrt{L_e^* C_e^*} \quad . \tag{2.57}$$

The above equation represents the dispersion relation. On substituting the value of series inductance per unit length (L_e^*) and shunt capacitance per unit length (C_e^*) and rearranging, the dispersion relation is written as:

$$\sum_{n=-\infty}^{\infty} (\xi_{n,m}^I - \xi_{n,m}^{II}) = 0 \quad . \tag{2.58}$$

The above dispersion relation (2.58) is the same as derived using a more involved and cumbersome field analysis approach, where

$$\xi_{n,m}^I = \frac{\cos(\beta_m^{III} d)}{2\pi \mathrm{r}_d(d)} \times \left[\frac{X_0\left\{\gamma_m^{III} r\right\}}{\phi_n(1-bJ_0\left\{\gamma_n r_b\right\}Y_0\left\{\gamma_n r_b\right\})J_0\left\{\gamma_n r\right\} + bJ_0^2\left\{\gamma_n r_b\right\}Y_0\left\{\gamma_n r\right\}}\right],$$

$$\xi_{nm}^{II} = \frac{\cos(\beta_m^{III}(d))}{2\pi \mathrm{r}_d(j\omega\varepsilon)(d)} \times \frac{\gamma_n}{\phi_n}\left[\frac{X_0'\left\{\gamma_m^{III} r\right\}}{(1-bJ_0\left\{\gamma_n r_b\right\}Y_0\left\{\gamma_n r_b\right\})J_1\left\{\gamma_n r\right\} + bJ_0^2\left\{\gamma_n r_b\right\}Y_1\left\{\gamma_n r\right\}}\right].$$

The dispersion relation for RF interaction structure is obtained here, on applying the equivalent circuit approach, and is used to plot the dispersion characteristics as well as study the role of structural parameters to control its shape. For finding the temporal growth rate, Eq. (2.58) is differentiated with respect to ω, by substituting $\omega \to \omega_0 + \delta\omega$, on rearranging results:

$$\delta\omega = -\omega + [(\frac{\gamma_n}{j\varepsilon}\phi_n \frac{X_0'\{\gamma_m^{III} r\}}{X_0\{\gamma_m^{III} r\}} \times (\frac{1 - bJ_0\{\gamma_n r_b\}Y_0\{\gamma_n r_b\})J_0\{\gamma_n r\} + bJ_0^2\{\gamma_n r_b\}Y_0\{\gamma_n r\}}{1 - bJ_0\{\gamma_n r_b\}Y_0\{\gamma_n r_b\})J_1\{\gamma_n r\} + bJ_0^2\{\gamma_n r_b\}Y_1\{\gamma_n r\}})]^{1/2} \tag{2.59}$$

The above equation represents expression for temporal growth rate (that is the imaginary part of ω, which shows that waves are unstable and they grow in amplitude, drawing energy from the sheared velocity field of relativistic Brillouin flow.

(viii). RF Power and Energy

In this section, RF energy stored and transferred through the slow-wave structure is calculated using an equivalent circuit approach. The admittance of the cavity [Dwivedi and Jain (2014)] can be written as:

$$Y(\omega) = \frac{1}{R}\left[1 + jRC\omega_0\left(\frac{\omega}{\omega_0} - \frac{\omega_0}{\omega}\right)\right]$$

$$Y(\omega) = \frac{1}{R}\left[1 + jQ_{\text{int}}\left(\frac{\omega}{\omega_0} - \frac{\omega_0}{\omega}\right)\right], \tag{2.60}$$

where, $Q_{\text{int}} = RC\omega_0$ represents the over-voltage coefficient or internal quality factor of a cavity, due to dissipative losses in the walls [Cousin *et al.* (2005)]. The imaginary part of admittance represents energy stored or released from the cavity. Due to resonant frequency ω_0, the external over-voltage coefficient or external quality factor is written

as, $Q_{ext} = \frac{Z_0}{\omega_0 L} = Z_0 C \omega_0$, here, Z_0 represents output impedance of the signal source. In MILO, energy stored inside the cavity is coupled with the load through a coaxial line with the output opening axially [Cousin *et al.* (2005)]. Interaction cavities coupling with the load may be either over coupling or under coupling depends upon the external and internal Q-factor. The coupling coefficient of the cavity is defined as,

$$\frac{Q_{ext}}{Q_{\text{int}}} = \frac{Z_0}{R} = \alpha \,. \tag{2.61}$$

For impedance matching, if a transmission line is connected between source and load together, it must also be the same impedance, $Z_0 = Z_i = Z_c$, where Z_c is the coupling impedance of the transmission line. During resonance when, $\alpha = 1$, $Z_c = Z_0$, the output guide is adapted with cavity and system behaves like an equivalent resonator or all electromagnetic energy injected is dissipated in cavity equivalent resistance.

Power transferred with the load is written as:

$$P = P_0(1 - \rho\bar{\rho}) \quad , \tag{2.62}$$

where, P_0 is initial power injected and ρ represents a complex reflection coefficient function of the load impedance Z_c and guide characteristic impedance Z_0 such as,

$$\rho = \frac{Z_0 - Z_c}{Z_0 + Z_c} = \frac{Y_c - Y_0}{Y_c + Y_0} \quad . \tag{2.63}$$

Substituting Eqs. (2.60) and (2.61) in (2.63),

$$\rho = \frac{(\alpha^2 - 1) + \alpha^2 Q_{\text{int}}^2 (\frac{\omega}{\omega_0} - \frac{\omega_0}{\omega})^2 + 2j\alpha Q_{\text{int}} (\frac{\omega}{\omega_0} - \frac{\omega_0}{\omega})}{(\alpha + 1)^2 + \alpha^2 Q_{\text{int}}^2 (\frac{\omega}{\omega_0} - \frac{\omega_0}{\omega})^2} \quad . \tag{2.64}$$

Multiply Eq. (2.64) by its complex and after simple algebra, we get

$$(1-\rho\bar{\rho}) = \frac{P}{P_0} = \frac{4\alpha}{(\alpha+1)^2 + \alpha^2 Q_{\text{int}}^2 (\frac{\omega}{\omega_0} - \frac{\omega_0}{\omega})^2} . \tag{2.65}$$

Eliminating α from the expression,

$$\frac{P}{P_0} = \frac{4(Q_{ext} / Q_{\text{int}})}{(1+Q_{ext} / Q_{\text{int}})^2 + Q_{ext}^2 (\frac{\omega}{\omega_0} - \frac{\omega_0}{\omega})^2} \quad . \tag{2.66}$$

Empty over-voltage coefficient,

$$Q_0 = \omega_0 \frac{W}{dW/dt}$$

$$\frac{P}{P_0} = \frac{4Q_{ext}(\frac{1}{Q_{\text{int}}} + \frac{1}{\omega_0 W}\frac{dW}{dt})}{[1+Q_{ext}(1/Q_{\text{int}} + 1/\omega_0 W(dW/dt)]^2 + Q_{ext}^2(\omega/\omega_0 - \omega_0/\omega)^2} . \tag{2.67}$$

Power seen by the cavity is the sum of the variation of energy stored during *dt* and of the power dissipated ($\omega_0 W / Q_{\text{int}}$) in the walls of the disc,

$$P = \frac{dW}{dt} + \frac{\omega_0 W}{Q_{\text{int}}}, \tag{2.68}$$

$$\frac{P}{\omega_0 W} = \frac{1}{Q_{\text{int}}} + \frac{1}{\omega_0 W}\frac{dW}{dt} \quad . \tag{2.69}$$

Eq. (2.69) can be rewritten after applying the condition of resonance,

$$P = \sqrt{\frac{4P_0\omega_0 W}{Q_{ext}}} - \frac{\omega_0 W}{Q_{ext}} . \tag{2.70}$$

Equating Eqs. (2.68) and (2.70), results in a first-order differential equation:

$$\frac{dW}{dt} + \frac{\omega_0}{Q_0} W - \sqrt{\frac{4P_0\omega_0}{Q_{ext}}}\sqrt{W} = 0 . \tag{2.71}$$

Dividing the above equation by ($W^{1/2}$), the above equation becomes,

$$\frac{d(W^{1/2})}{dt}+\frac{\omega_0}{2Q_0}W^{1/2}-\sqrt{\frac{P_0\omega_0}{Q_{ext}}}=0 \quad . \tag{2.72}$$

The general solution of the above expression,

$$W(\mathrm{t})=\frac{4P_0Q_0^2}{\omega_0 Q_{ext}}\left[1-\exp\left(-\left(\frac{\omega_0}{2Q_0}t\right)\right)\right]^2, \tag{2.73}$$

$$W(t)=W_0\left[1-\exp\left(-\frac{\omega_0}{2Q_0}t\right)\right]^2. \tag{2.74}$$

Here, $\omega_0=1/\sqrt{L_eC_e}$ and $W_0=4P_0Q_0^2/\omega_0Q_{ext}$. Q_0 is the loaded quality factor and is proportional to energetic storage characteristic time inside the slow-wave structure [Cousin *et al.* (2005)]. W_0 is the maximum energy stored inside the resonator. RF energy developed through the MILO device is calculated using Eq. (2.74) on substituting equation for inductance and capacitance per unit length. Temporal RF output power developed during the beam-wave interaction process is calculated by substituting (2.74) in (2.70), thus released RF energy is used to calculate RF output power from the device.

2.5. Conclusion

In this chapter, the equivalent circuit approach which is used to study beam wave interaction analysis for periodic disc loaded coaxial structure used in the MILO device has been reviewed and described in details. For this, firstly, various analytical approaches that have been used in analysing such structures so far have been reviewed. Then, the equivalent circuit analysis for MILO in the beam absent case has been

discussed and various characteristics of periodic disc loaded coaxial structure such as dispersion relation, phase velocity, and characteristic impedance has been derived using equivalent line parameters. To derive these characteristics, the actual structure has been replaced by an equivalent transmission line in terms of its equivalent circuit parameters with the assumption of the loss-free condition. The two-line parameters (i.e. the series inductance and shunt capacitance per unit length) of the line have been used for analysis. These two parameters are derived independently and one has to deal with only half of the total structure EM field expressions and boundary conditions at a time which makes the analysis simpler and yields relatively much simple expression. The dispersion characteristics obtained by the present equivalent circuit approach exactly pass to those expressions which were obtained through the field analysis. The characteristic impedance of the line in the beam absent case which is an important parameter while considering circuit matching condition is also be obtained through the present analysis. Furthermore, the equivalent circuit analysis for MILO in the beam present case has been discussed. The equivalent circuit approach has been developed in this chapter considering the presence of an electron beam in order to study the RF analysis of MILO. This approach has been used to investigate the device oscillation condition, dispersion relation, and temporal RF growth rate.

The equivalent circuit approach which was used by different researchers earlier was encumbered and having limitation to decipher the device behavior. Like, Fan *et al.* had used the equivalent circuit approach to analyze the periodic disc-loaded coaxial structure for fundamental modes only. The problem associated with this approach is that one cannot analyze the structure behavior for the higher order modes. The equivalent circuit approach used by Dixit *et al.* had limited their analysis for azimuthally

symmetric structures and for only symmetric TM_{0n} modes. The problem associated with this approach is that we cannot perform the complete analysis (i.e., like symmetric TE mode and asymmetric modes supported by the structure) of coaxial structure. Here, the equivalent circuit approach used in this thesis can be used to analyze for both symmetric as well as asymmetric modes supported in the coaxial structures. Also, the present approach can be used for all kind of coaxial structure which is either be azimuthally symmetric or azimuthally partitioned. Therefore, this approach eliminates the limitation of previously developed equivalent circuit approach.